LIMNOLOGY
and
OCEANOGRAPHY: METHODS

Limnol. Oceanogr.: Methods 10, 2012, 142–154

Direct estimation of functional PSII reaction center concentration and PSII electron flux on a volume basis: a new approach to the analysis of Fast Repetition Rate fluorometry (FRRf) data

Kevin Oxborough[1], C. Mark Moore[2], David J. Suggett[3], Tracy Lawson[3], Hoi Ga Chan[1], and Richard J. Geider[3]*
[1]CTG Ltd., 55 Central Avenue, West Molesey, KT8 2QZ, UK
[2]Ocean and Earth Science, University of Southampton, National Oceanography Centre, Southampton, SO14 3ZH, UK
[3]School of Biological Sciences, University of Essex, CO4 3SQ, UK

Abstract

Phytoplankton primary productivity is most commonly measured by ^{14}C assimilation although less direct methods, such as O_2 exchange, have also been employed. These methods are invasive, requiring bottle incubation for up to 24 h. As an alternative, Fast Repetition Rate fluorometry (FRRf) has been used, on wide temporal and spatial scales within aquatic systems, to estimate photosystem II (PSII) electron flux per unit volume (JV_{PSII}), which generally correlates well with photosynthetic O_2 evolution. A major limitation of using FRRf arises from the need to employ an independent method to determine the concentration of functional photosystem II reaction centers ([RCII]); a requirement that has prevented FRR fluorometers being used, as stand-alone instruments, for the estimation of electron transport. Within this study, we have taken a new approach to the analysis of FRRf data, based on a simple hypothesis; that under a given set of environmental conditions, the ratio of rate constants for RCII fluorescence emission and photochemistry falls within a narrow range, for all groups of phytoplankton. We present a simple equation, derived from the established FRRf algorithm, for determining [RCII] from dark FRRf data alone. We also describe an entirely new algorithm for estimating JV_{PSII}, which does not require determination of [RCII] and is valid for a heterogeneous model of connectivity among RCIIs. Empirical supporting evidence is presented. These data are derived from FRR measurements across a diverse range of microalgae, in parallel with independent measurements of [RCII]. Possible sources of error, particularly under nutrient stress conditions, are discussed.

Direct measurement of gross photosynthesis and primary productivity

The rate of photosynthesis is a primary constraint on the availability of energy for the production of organic matter within aquatic ecosystems. Gross photosynthesis (GP) is defined as the rate at which reducing power is generated through the conversion of absorbed light energy, with the assumption that most of this energy is used for organic matter production (gross primary productivity (GPP); Begon et al. 2006). For example, Raven (2009) estimated that oxygenic photosynthesis contributes greater than 99% of global GPP. The distinction between GPP and GP is necessary, as a number of processes operating between O_2 evolution at photosystem II (PSII) and CO_2 assimilation by the Calvin cycle can uncouple GPP from GP (Geider and MacIntyre 2002; Behrenfeld et al. 2004; Halsey et al. 2010; Suggett et al. 2010a). GPP or GP is often reported per unit area of lake, stream, or ocean surface, or per unit volume of water. Within the oxygenic photoautotrophs, which includes the phytoplankton that dominate most aquatic environments, O_2 is generated as a by-product of GP. Thus, GPP can be reported as carbon assimilation (e.g., as mol C m^{-3} d^{-1} or mol C m^{-2} d^{-1}), whereas GP can be reported as oxygen evolution (e.g., as mol O_2 m^{-3} d^{-1} or mol O_2 m^{-2} d^{-1})

*Corresponding author: E-mail: koxborough@chelsea.co.uk

Acknowledgments

We would like to thank Tania Cresswell-Maynard (University of Essex) for providing many of the cultures used within this study and Kimberley Walrond (University of Manchester) for helpful discussions.
Contributions of DJS and RJG were supported by the EU project PROTOOL (EU-226880). The contribution of CMM was supported by the Natural Environment Research Council, UK (NE/G009155/1). The authors owe extreme thanks to Hugh MacIntyre (Dalhousie University, Halifax, Canada) and Marie-Hélène Forget (Bedford Institute of Oceanography, Dartmouth, Canada) for their assistance and contributions in facilitating the Mk I FAST*tracka* data sets evaluated here.

DOI 10.4319/lom.2012.10.142

or PSII electron transport (e.g., mol e^- m^{-3} d^{-1} or mol e^- m^{-2} d^{-1}). For the phytoplankton, GPP is most commonly quantified using ^{14}C incorporation, with O_2 exchange being widely employed as a proxy for GP (Bender et al. 1987). Both methods are invasive, requiring that samples be incubated in bottles for up to 24 h, with attendant bottle effects (Venrick et al. 1977; Fogg and Calvario-Martinez, 1989).

Indirect measurement of gross photosynthesis using active fluorescence

Active fluorometry has been adopted widely by the scientific community and ecosystem managers, predominantly as a nonintrusive technique for probing photosynthesis and other physiological processes within phytoplankton and benthic autotrophs, including corals and sea grasses (Suggett et al. 2010b). In a wide range of studies, active fluorometry has successfully been used to compliment other techniques, on scales ranging from the molecular to ecosystem (e.g., Falkowski and Kiefer 1985; Falkowski et al. 1991; Moore et al. 2003; Behrenfeld et al. 2006; Suggett et al. 2009b). However, the use of active fluorometry to estimate GP or infer GPP, alone or in combination with other techniques, has been constrained by both procedural inconsistencies and inherent assumptions within the algorithms used to estimate photosynthetic electron transport (see Suggett et al. 2009a, 2010a). As a consequence, active fluorometry has not fully lived up to expectations, either as a 'productivity meter' or as a management tool for the rapid assessment of ecosystem viability.

Fast Repetition Rate fluorometry (FRRf) is a widely used variant of active fluorometry, which has frequently been employed for the in situ estimation of GP from optically thin material, over a wide range of temporal and spatial scales (Kolber and Falkowski 1993; Kolber et al. 1998; Moore et al. 2006; Suggett et al. 2001; Suggett et al. 2009b). FRRf allows direct calculation of the absorption cross section of PSII photochemistry (σ_{PSII} in the dark-adapted state, σ_{PSII}' under ambient light) through an iterative curve fit to the saturation phase of an FRRf single turnover (ST) measurement (Fig. 1). Importantly, the value of σ_{PSII} or σ_{PSII}' derived from the iterative curve fit is valid for functional PSII reaction centers (RCIIs) that are open at the zeroth flashlet of an ST measurement (at F_o in the dark-adapted state or F' under ambient light, see Table 1). Consequently, the product of σ_{PSII}', with units of m^2, and incident photosynthetically active radiation (E), with units of photons m^{-2} s^{-1}, provides an estimate of photochemical flux through each open RCII (J_{PSII}), with units of photons s^{-1} or (assuming an efficiency of one charge-separation event per photon) with units of electrons s^{-1} (Eq. 1).

$$J_{PSII} = \sigma_{PSII}' \cdot E \qquad (1)$$

To make use of J_{PSII} in the estimation of GP, both the concentration of functional PSII reaction centers ([RCII]) and the fraction of RCII in the open state must be determined (Falkowski and Kiefer 1985; Kolber and Falkowski, 1993). This

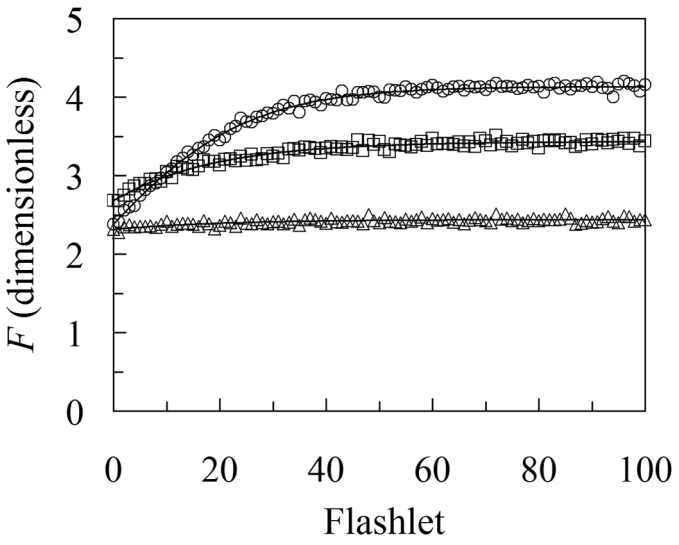

Fig. 1. Three ST acquisitions from an optically thin static sample of *Emiliania huxleyi* under different ambient light levels. All three acquisitions comprise 24 sequences, collected with 100 ms between adjacent sequences. One microsecond flashlets were delivered on a 2 µs pitch, giving a total time of 200 µs for each sequence. Each symbol represents an average from the 24 sequences. The solid lines are iterative fits through the entire ST curve (Kolber et al. 1989). E = 21 (open circles), 263 (open squares), or 1202 (open triangles) µmol photons m^{-2} s^{-1}.

allows calculation of the PSII charge separation rate per unit volume (JV_{PSII}), with units of electrons m^{-3} s^{-1}, using Eq. 2 (Kolber and Falkowski, 1993; Suggett et al. 2010a).

$$JV_{PSII} = J_{PSII} \cdot [\text{RCII}] \cdot (1 - C) = \sigma_{PSII}' \cdot [\text{RCII}] \cdot (1 - C) \cdot E \qquad (2)$$

where E has units of photons m^{-2} s^{-1}, [RCII] is the concentration of functional PSII reaction centers (m^{-3}), C is the fraction of RCII in the closed state (Q_A reduced, incapable of stable charge separation), and consequently, $1 - C$ is the fraction of RCII in the open state (Q_A oxidized, capable of stable charge separation).

A major limitation of using FRRf to measure JV_{PSIII} arises from the need for an independent method to determine [RCII]; a requirement that clearly limits the utility of FRR fluorometers as stand-alone instruments. Typically, [RCII] has been derived from direct measurement of chlorophyll *a* concentration, under the assumption that the total number of Chl *a* molecules associated with both PSII and photosystem I (PSI) per RCII is relatively constant (Kolber and Falkowski 1993; Suggett et al. 2001). Aside from the need for an independent measurement of Chl *a* on a discrete sample, a weakness of this approach is that the number of RCII per chlorophyll (frequently denoted as n_{PSII}) shows considerable taxonomic and physiological variability (Suggett et al. 2004). In addition, the limited data available from natural phytoplankton communities provides similar evidence of considerable in situ variability for this parameter (Moore et al. 2006; Suggett et al. 2006).

Table 1. Terms used within this manuscript.

Term	Description	Units
a_{LHII}	LHII absorption coefficient	m^{-1}
E	incident photosynthetically active radiation	photons m^{-2} s^{-1}
E_{LED}	photon output from the FRRf measuring LEDs	photons m^{-2} s^{-1}
F'	fluorescence at zeroth flashlet of an ST measurement when $C > 0$	dimensionless
$F_o^{(\prime)}$	fluorescence at zeroth flashlet of an ST measurement when $C = 0$ (under ambient light)	dimensionless
$F_m^{(\prime)}$	fluorescence when $C = 1$ (under ambient light)	dimensionless
F_q'	$F_m' - F'$	dimensionless
$F_v^{(\prime)}$	$F_m^{(\prime)} - F_o^{(\prime)}$	dimensionless
$F_v^{(\prime)}/F_m^{(\prime)}$	fluorescence parameter providing an estimate of ϕ_{PSII} when $C = 0$ (under ambient light)	dimensionless
GP	Gross photosynthesis	
GPP	Gross primary productivity	
K_N	Cross-compatible value of K_R, derived through normalization of the fluorescence signal	photons s^{-1}
K_R	Instrument specific constant, which allows for direct calculation of [RCII] and JV_{PSII} from FRR data	photons m^{-3} s^{-1}
ϕ_{PSII}	PSII quantum efficiency	
ST	Single turnover, fast repetition rate acquisition	
FRRf	Fast Repetition Rate fluorometer/fluorometry	
oF'	fluorescence from open centers under ambient light	dimensionless
J_{PSII}	PS II flux	electrons s^{-1}
JV_{PSII}	PSII flux per unit volume	electrons m^{-3} s^{-1}
[RCII]	concentration of functional PS II reaction centers	m^{-3}
σ_{LHCII}	absorption cross section of PSII light harvesting	m^2
σ_{PSII}	absorption cross section of PSII photochemistry	m^2

Although the need to generate a value for [RCII] imposes the greatest limitation to the application of Eq. 2, generating a value of σ_{PSII}' also can present significant practical challenges. As already noted, a value for σ_{PSII}' is derived from an iterative curve fit to the variable fluorescence signal ($F_q' = F_m' - F'$, see Table 1 for terms used) during an ambient light ST measurement (Fig. 1).

With increasing ambient light, F_q' tends to decrease. This is due to an increase in F', caused by closure of RCII, coupled with a preferential decrease in F_m', due to an increase in nonphotochemical quenching (reviewed by Baker and Oxborough 2004; Krause and Jahns 2004). Ultimately, this can prevent a reliable fit being made at high levels of ambient light. The data presented in Fig. 2 show light-dependent changes in F_q' and σ_{PSII}' within an optically thin static sample of *Emiliania huxleyi*. Within this example, F_q' decreased by a factor of ten as E was increased from 0 to 1202 µmol photons m^{-2} s^{-1} during a so-called rapid light curve (RLC). Although there was very little change in the mean value of σ_{PSII}', between 0 and 1202 µmol photons m^{-2} s^{-1}, there was a large increase in the uncertainty, as F_q' decreased to a small proportion of the total fluorescence signal.

An additional complicating factor arising from Eq. 2 is the degree of connectivity among RCIIs. Under ambient light, connectivity results in the net transfer of excitation energy from closed to open RCIIs (Joliot and Joliot 1964; Lavergne and Trissl 1995; Kolber et al. 1998), which has implications for the calculation of $1 - C$. The most widely used parameter for estimating $(1 - C)$ in Eq. 2 is qP (e.g., Kolber et al. 1998; Suggett et al. 2001, 2004), which assumes zero connectivity between adjacent RCIIs. Although there are alternative param-

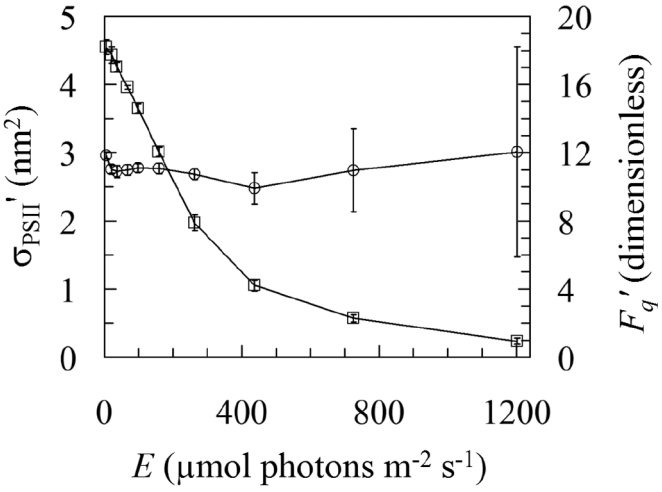

Fig. 2. Values of σ_{PSII}' (open circles) and F_q' (open squares) from an optically thin static sample of *Emiliania huxleyi*. Shown are the mean values, plus 95% confidence intervals for $n = 10$. Data were collected during an RLC sequence, during which E was increased from 0 to 1202 µmol photons m^{-2} s^{-1}. Acquisitions were made at 20-s intervals. Further details are provided in the legend to Fig. 1.

eters for estimation of (1 – *C*), which assume either perfect connectivity among all RCIIs within the sample (Kramer et al. 2004) or a uniform, intermediate level of connectivity, these provide (at best) only a marginal advantage over qP. A discussion of the options available for calculating 1 – *C* is provided within Web Appendix A to this manuscript.

Within this study, we present a simple equation for the calculation of [RCII] from dark ST data. This equation, which incorporates σ_{PSII}, is derived from the established FRRf algorithm, as originally presented by Kolber and Falkowski (1993). Although this development allows Eq. 2 to be used without independent determination of [RCII], we also present an entirely new algorithm for calculating JV_{PSII} from ST data that does not require that values for [RCII], σ_{PSII}' or 1 – *C* and does not require that any assumptions are made with regard to the type or extent of connectivity among RCIIs.

This new approach to the analysis of FRRf data incorporates one basic hypothesis; that under a given set of environmental conditions, the ratio of rate constants for photochemistry (k_p) and fluorescence (k_f) at open RCIIs falls within a narrow range, for all groups of phytoplankton. There are two important consequences to this hypothesis: (1) The number of RCII is proportional to fluorescence emitted from open RCII divided by the absorption cross section of PS II photochemistry (σ_{PSII}). (2) The fluorescence emitted from open RCIIs under ambient light is proportional to JV_{PSII}.

The equation for calculating [RCII] takes advantage of (1), whereas the new algorithm for calculating JV_{PSII} takes advantage of (2).

The established FRRf algorithm (hereafter, the sigma algorithm) assumes that connectivity among RCIIs is uniform and that open RCIIs within a sample do not have widely divergent values of σ_{PSII}. In contrast, the new algorithm (hereafter, the absorption algorithm) makes no such assumption and is entirely compatible with a wide range of values for σ_{PSII} within the sample. The consequences of the important differences between the algorithms are covered within the remainder of this section. Later sections deal with practical implementation of the new equation for calculating [RCII] and the absorption algorithm and include examples from field- and laboratory-based studies. A description of the terms used within this manuscript is provided within Table 1.

Theory: Open or Closed RCIIs

Within an isolated RCII in the open state, the quantum yields of fluorescence (ϕ_f) and photochemistry (ϕ_p) are dependent on the rate constants for photochemistry (k_p), fluorescence (k_f), and nonradiative decay (k_d), such that:

$$\varphi_f = \frac{k_f}{k_p + k_f + k_d} \tag{3a}$$

$$\varphi_p = \frac{k_p}{k_p + k_f + k_d} \tag{3b}$$

From Eqs. 3a and 3b, it is clear that k_d has a proportional impact on the values of ϕ_f and ϕ_p. Consequently, if k_f/k_p remains constant, any change in ϕ_f will result in a proportional change in ϕ_p.

In contrast, the value of k_p at a closed center is zero, such that:

$$\varphi_f = \frac{k_f}{k_f + k_d} \tag{4a}$$

$$\varphi_p = 0 \tag{4b}$$

It follows that, for population of open RCIIs within an optically thin sample in the dark-adapted state, the measured fluorescence emission (F_o or F_o') is provided by:

$$F_o^{(')} \propto \frac{k_f}{k_p + k_f + k_d} \cdot [\mathrm{RCII}] \cdot \sigma_{\mathrm{LHII}} \tag{5a}$$

where [RCII] is the concentration of RCIIs within the sample and σ_{LHII} is the absorption cross section of the light harvesting system associated with each RCII, with units of m^2. It should be noted that $[RCII]\cdot\sigma_{LHII}$ within Eq. 5a represents an absorption coefficient for PSII light harvesting (hereafter, a_{LHII}), with units of m^{-1}. Consequently,

$$F_o^{(')} \propto \frac{k_f}{k_p + k_f + k_d} \cdot a_{\mathrm{LHII}} \tag{5b}$$

whilst, for a population of closed RCIIs, the measured fluorescence (F_m or F_m') is provided by:

$$F_m^{(')} \propto \frac{k_f}{k_f + k_d} \cdot a_{\mathrm{LHII}} \tag{6}$$

Theory: Derivation of the Sigma Algorithm-Based Equation to Provide [RCII]

The absorption cross section of PSII photochemistry (σ_{PSII}) is the product of σ_{LHII} and the quantum yield of PSII photochemistry, ϕ_p (see Eq. 3b). Consequently, we can derive:

$$\sigma_{\mathrm{PSII}} = \sigma_{\mathrm{LHII}} \cdot \frac{k_p}{k_p + k_f + k_d} \tag{7}$$

as originally presented by Kolber et al. (1998). From Eqs. 5a and 7, it is evident that

$$F_o \propto \frac{k_f}{k_p} \cdot [\mathrm{RCII}] \cdot \sigma_{\mathrm{PSII}} \tag{8}$$

and that

$$[\mathrm{RCII}] \propto \frac{k_p}{k_f} \cdot \frac{F_o}{\sigma_{\mathrm{PSII}}} \tag{9}$$

Consequently, if k_f/k_p is constant, it is clear that [RCII] is proportional to F_o/σ_{PSII}. We therefore can derive

$$[\mathrm{RCII}] = \frac{\mathrm{K_R}}{E_{\mathrm{LED}}} \cdot \frac{F_o}{\sigma_{\mathrm{PSII}}} \tag{10a}$$

where K_R is an instrument-specific constant, with units of photons m^{-3} s^{-1}.

In practice, the value of K_R can be determined by calibration against simultaneous measurements of [RCII] and σ_{PSII} as follows:

$$K_R = [RCII] \cdot \frac{\sigma_{PSII}}{F_o} \cdot E_{LED} \quad (10b)$$

where E_{LED} is the measuring beam intensity, with units of photons m^{-2} s^{-1}, and F_o is dimensionless.

Theory: Derivation of Absorption Algorithm

There is a substantial body of evidence from studies with vascular plants and macroalgae to show that the rate of PSII electron transport is proportional to F_q'/F_m', where $F_q' = F_m' - F'$, as originally described by Genty et al. (1989). When working with optically dense material, such as the leaves of vascular plants or fronds of macroalgae, an integrating sphere can often be used to determine the number of photosynthetically active photons absorbed per unit area, per unit time, with a high degree of confidence. Given that GP is the product of PSII quantum efficiency (ϕ_{PSII}) and photons absorbed by PSII, this makes it possible to estimate GP, by assuming 50% of photons are absorbed by PSII, with the remaining 50% assumed by PSI (reviewed by Baker and Oxborough 2004).

To make use of F_q'/F_m' when working with optically thin samples of algae, we need to determine the number of photosynthetically active photons absorbed by PSII per unit volume, per unit time. To this end, we can derive the following:

$$JV_{PSII} = \frac{F_q'}{F_m'} \cdot a_{LHII} \cdot E \quad (11)$$

Since routine, direct measurement of a_{LHII} from an optically thin target is not a practical proposition, we require a method of generating a proxy value for this parameter. Combining Eqs. 5b and 6, we can derive

$$\frac{F_m \cdot F_o}{F_m - F_o} \propto \frac{k_f}{k_p} \cdot a_{LHII} \quad (12a)$$

$$a_{LHII} = \frac{F_m \cdot F_o}{F_m - F_o} \cdot \frac{K_R}{E_{LED}} \quad (12b)$$

With the value of the proportionality constant (K_R) being the same as in Eq. 10b, substituting the righthand side of Eq. 12b into Eq. 11 provides:

$$JV_{PSII} = \frac{F_m \cdot F_o}{F_m - F_o} \cdot \frac{F_q'}{F_m'} \cdot \frac{K_R}{E_{LED}} \cdot E \quad (13)$$

Effectively, Eqs. 12b and 13 comprise the absorption algorithm. From these equations, it is clear that calculation of a_{LHII} only requires values of F_o and F_m from dark FRRf data, whereas JV_{PSII} additionally requires F' and F_m' from ambient light FRRf data.

Theory: Isolating the Fluorescence Emitted from Open RCII under Ambient Irradiance (*oF'*)

To compare the sigma and absorption algorithms, it is instructive to return to Eqs. 3a and 3b, which illustrate the proportional impact of changes in k_d on both ϕ_f and ϕ_p, within an open RCII. A clear consequence of this relationship is that changes in k_d will have a proportional effect on F_o (which is proportional to ϕ_f) and F_v/F_m (which is proportional to ϕ_p). Assuming the k_p/k_f ratio is conserved when moving from the dark adapted state to ambient light, linearity between fluorescence emission and photochemistry by functional RCIIs in the open state must also be maintained. It follows that the fluorescence emitted from RCIIs under ambient light, which we define as *oF'*, will be proportional to JV_{PSII}/E, such that

$$JV_{PSII} = oF' \cdot \frac{K_R}{E_{LED}} \cdot E \quad (14)$$

Although *oF'* is not essential for the calculation of JV_{PSII}, using either algorithm, this parameter provides a useful construct for illustrating the difference in the way that connectivity among RCIIs is handled by each algorithm.

Generating a sigma algorithm–based value of *oF'* is straightforward. Given that, in the dark-adapted state, the fluorescence emitted by open RCIIs is provided by F_o and the fluorescence emitted by each open RCII changes in proportion to σ_{PSII}, we can derive:

$$oF' = F_o \cdot \frac{\sigma_{PSII}'}{\sigma_{PSII}} \cdot (1 - C) \quad (15)$$

An absorption algorithm–based value of *oF'* can be derived from Eqs. 13 and 14:

$$oF' = \frac{F_m \cdot F_o}{F_m - F_o} \cdot \frac{F_q'}{F_m'} \quad (16)$$

Within Eq. 15, $\sigma_{PSII}'/\sigma_{PSII}$ accounts for any change in σ_{PSII} between the dark-adapted state and under ambient light, whereas $(1 - C)$ represents the fraction of RCIIs in the open state. As already noted, the value of $(1 - C)$ depends on the connectivity model used for the calculation (see Web Appendix A for a discussion). The value of $\sigma_{PSII}^{(\prime)}$ is also affected by the connectivity model used, though to a much smaller extent. In contrast, neither of the terms within Eq. 16 require any assumptions regarding connectivity among RCIIs: $F_m \cdot F_o/(F_m - F_o)$ only requires values of F_o and F_m, whereas F_q'/F_m' provides an estimate of $\phi_{PSII,}$ which is valid for any model of connectivity (see Web Appendix A for a discussion).

Theory: Cross-calibration among Fluorometers

The derivation of K_R (Eqs. 10a and 10b) incorporates the instrument-specific, dimensionless value of F_o. Direct, cross-compatibility of K_R among FRR fluorometers requires that the following criteria are satisfied: (1) The spectral output of the instrument LEDs used to generate the fluorescence signal are identical. (2) A specific sample generates the same numeric value of F_o at a specified gain setting.

Although (1) is normally satisfied among fluorometers of the same model, even small differences in sensor sensitivity and/or optical efficiency can result in significant differences in the value of F_o at the same gain setting.

Providing (1) is satisfied, a simple way of implementing cross-compatibility is to normalize the F_o signal to an easily implemented standard, such as a known concentration of chl *a* in acetone ([Chl]):

$$K_R = K_N \cdot \frac{[Chl]}{F_{Chl}} \quad (17)$$

where K_N is a normalized, cross-compatible value of K_R, with units of photons s^{-1}, [Chl] is a known concentration of Chl *a* molecules in acetone, with units of m^{-3}, and F_{Chl} is the fluorescence signal generated by [Chl] at a specific gain setting. Given the ease with which this measurement can be made, it is clearly much more practical to cross-calibrate using K_N, rather than making individual measurements of [RCII] or JV_{PSII} for each fluorometer.

Materials and procedures

[RCII] examples

The Mk I FAST*tracka* fluorometers used for the Bedford Basin (BB) and Horn Point (HP) studies were manufactured by CTG Ltd. The serial numbers and relevant calibration information for these units are provided in Table 2.

All [RCII] measurements, within both studies, were made using the same purpose-built O_2 flash yield system (described by Suggett et al. 2009a). For these measurements, cells were concentrated by gentle reverse filtration (BB study) or gravity filtration (HP study) to a final Chl *a* concentration of between 1 and 5 nM. FRRf was used to verify that the photo-physiological status of the cells was not affected by the concentration procedure (Moore et al. 2006).

Chl *a* concentrations from samples, before and after the concentration of cells, were determined using the nonacidification technique (Welschmeyer 1994) after extraction in 90% acetone (BB study) or a mix of 90% acetone and dimethyl sulfoxide (HP study; Shoaf and Lium 1976).

Table 2. Calibration information for the Mk I FAST*tracka* fluorometers used within the BB and HP studies. [RCII], σ_{PSII}, and F_o are mean values from all samples within each study. Values of E_{LED} and F_{Chl}/[Chl] are derived from the calibration certificate for each fluorometer. The difference between the K_R values is 8.8%, while the difference between the K_N values is 6.2% (both referenced to the HP values). All terms are defined within Table 1.

	Bedford Basin (BB)	Horn Point (HP)
Mk I FAST*tracka* serial number	182042	182027
[RCII] (m^{-3})	7.657×10^{15}	2.905×10^{17}
σ_{PSII} (m^2)	3.46×10^{-9}	5.979×10^{-9}
F_o (gain corrected, dimensionless)	0.2237	5.07
E_{LED} (photons m^{-2} s^{-1})	1.87×10^{13}	7.98×10^{12}
K_R (photons m^{-3} s^{-1})	2.36×10^{21}	2.59×10^{21}
F_{Chl}/[Chl] (m^{-3})	0.02232	0.02168
K_N values (photons s^{-1})	5.27×10^{19}	5.62×10^{19}

JV_{PSII} examples

All measurements were made using FAST*tracka* II fluorometers plus FAST*act* laboratory systems (both from CTG Ltd). The central emission wavelength of the fluorometer LEDs was 470 nm.

Assessment

Calculation of [RCII]

To test the validity of Eq. 10a, we have analyzed data collected from in situ phytoplankton communities and from cultures grown under controlled conditions. Assuming our hypothesis of a conserved k_p/k_f ratio holds, a close correlation should exist between [RCII] and F_o/σ_{PSII}.

The data presented in Figs. 3 and 4 were collected from two studies, using different Mk I FAST*tracka* FRRf fluorometers (CTG Ltd.). All [RCII] values within both studies were determined using a custom-built O_2 flash yield system, as described by Suggett et al. (2009a). The FRRf data, which are from standard ST measurements, were fitted using the model of Kolber et al. (1998). To allow for the calculation of K_N, values of E_{LED} were taken from the relevant calibration certificate, provided by the manufacturer.

The first set of data (Fig. 3) are from a field-based study conducted during a spring bloom (February 23rd to April 18th, 2005) in Bedford Basin, Canada, which was dominated by chain-forming diatoms of *Chaetoceros* sp. (hereafter, the BB data). These data are characterized by a wide range of chlorophyll concentrations (from 0.65 to 35 µmol m^{-3}), but a rela-

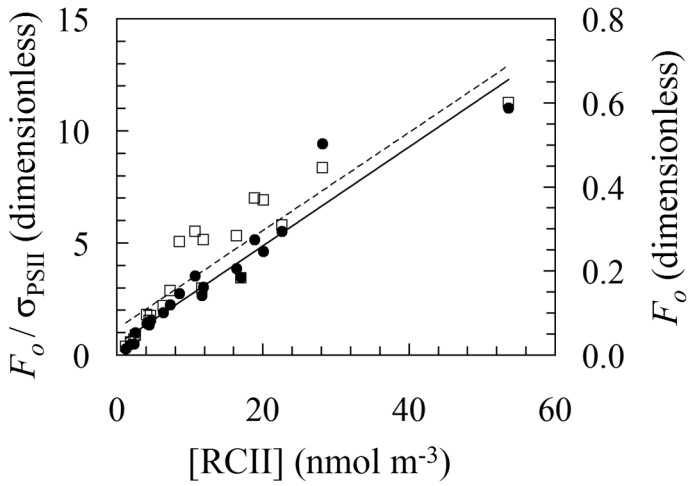

Fig. 3. Data collected from Bedford Basin, Canada, during a spring bloom, which was dominated by the diatom, *Chaetoceros* sp. Values for F_o/σ_{PSII} (closed circles) and F_o (open squares) are plotted against [RCII]. Linear regression generated R^2 values of 0.924 for F_o/σ_{PSII} (solid line) and 0.843 for F_o (dashed line). The intercept values (normalized to F_o/σ_{PSII}) were 0.45 for F_o/σ_{PSII} and 1.18 for F_o.

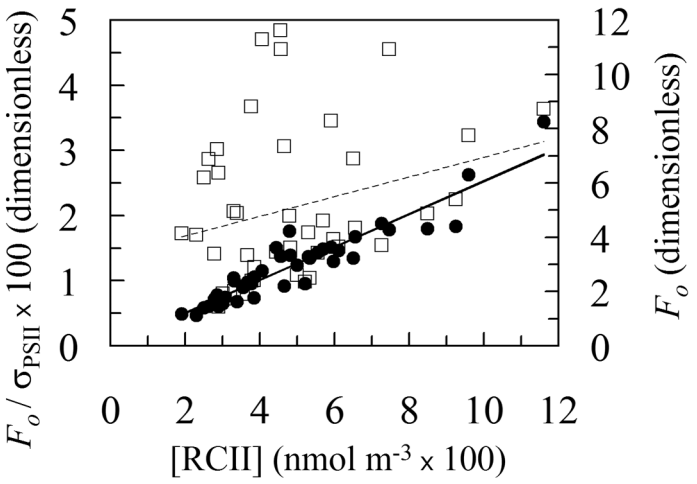

Fig. 4. Data from cultures of six species of microalgae, grown at three different light intensities. Values for F_o/σ_{PSII} (closed circles) and F_o (open squares) are plotted against [RCII]. Linear regression generated R^2 values of 0.869 for F_o/σ_{PSII} (solid line) and 0.0755 for F_o (dashed line). The intercept values (normalized to F_o/σ_{PSII}) were –1.06 for F_o/σ_{PSII} and 137.5 for F_o.

tively narrow range of values for σ_{PSII} (2.4 to 5.0 nm^2).

The second set of data (Fig. 4), which were published previously in a different format (Suggett et al. 2009a), are from a laboratory-based study conducted at Horn Point Laboratory, MD, U.S.A. (hereafter, the HP data). Included are measurements from six species, representing a broad taxonomic range of microalgae (*Aureococcus anophagefferens, Dunaliella tertiolecta, Prorocentrum minimum, Pycnococcus provasolii, Storeatula major*, and *Thalasiosira weissfloggii*), all of which were grown at three different light intensities (18, 80, and 300 µmol photons m^{-2} s^{-1}). In comparison with the BB data, the HP data include a relatively narrow range of chlorophyll concentrations (260 to 700 µmol m^{-3}) but a much wider range of values for σ_{PSII} (2.3 to 12.4 nm^2).

Strong correlations between [RCII] and F_o/σ_{PSII} are clearly evident within the data from both studies: approximately 90% of the variance being explained, with R^2 values of 0.924 and 0.869 for the BB data (Fig. 3) and HP data (Fig. 4), respectively. Importantly, linear regression generated an intercept that was very close to zero in both cases.

Clearly, a proportion of the observed correlation within the BB data could be forced by changes in overall phytoplankton biomass during the bloom, resulting in a parallel increase in both [RCII] and F_o. Indeed, changes in the fluorescence signal per se have been widely adopted as a proxy for phytoplankton chlorophyll (e.g., Falkowski and Kiefer 1985). To examine the extent to which the relationships between [RCII] and F_o/σ_{PSII} might have been forced in this way, we have included plots of [RCII] against F_o within Figs. 3 and 4. For the BB data set, although there is a strong correlation between [RCII] and F_o, the correction of F_o for differences in σ_{PSII} introduces a significant improvement, with the explained variance increasing from 0.843 to 0.924. The σ_{PSII} correction within the HP data are much more dramatic, with the explained variance increasing from an insignificant value of 0.0755 to 0.869 for the proposed new method.

The values of K_R and K_N for the BB and HP fluorometers are shown in Table 2. It is worth noting that, despite the difference in target material, the K_N values are within 6.2% of each other.

Calculation of JV_{PSII}

The validity of the sigma algorithm has already been tested extensively (Suggett et al. 2003, 2009a, 2010a). As a way of assessing the degree of equivalence between the sigma and absorption algorithms, values of *oF′* were calculated using both algorithms (Eqs. 15 and 16). To maintain consistency with earlier studies, the $1 - C$ values required within Eq. 15 were generated using qP (see Eq. A4 within Web Appendix A). The data used for this comparison are from a series of light response curve measurements, collected from six diverse species of phytoplankton (Fig. 5).

Perfect equivalence between the sigma and absorption algorithms would generate a slope of unity. Of the six species reported here, four are very close (regression slopes within 4%). The remaining two have slope values of 0.89 and 0.84, which are coupled with the lowest amount of variance (R^2 values of 0.90 and 0.87, respectively).

Perfect equivalence between the *oF′* values generated by the sigma and absorption algorithms would not be expected, given the differences in the way that connectivity among RCIIs is addressed within each algorithm. Nonetheless, it seems reasonable to conclude that these data demonstrate a high level of equivalence between the two algorithms.

Despite this statistical equivalence, there are regions within some plots that indicate a significant deviation from linearity. For example, the data points close to the origin within the *Emiliania huxleyi* and *Oscillatoria* plots are scattered below the regression line. The reason for these scattering points can clearly be seen within Fig. 6. Here, the product $oF' \cdot E$ (which should be directly proportional to JV_{PSII}) has been plotted against E, using values of *oF′* generated using the sigma and absorption algorithms. In every case, the scattering of data points away from the regression line is matched by large error bars for the sigma algorithm values.

It is worth noting that the error bars for the sigma algorithm values within the *Isochrysis galbana* plot of Fig. 6 overlap with the absorption algorithm mean values. Consequently, the slope of 0.84 within Fig. 5 does not actually represent a significant deviation from unity, and it is only the *Rhodomonas* data set that shows a significant difference between sigma algorithm and absorbance algorithm derived values of *oF′*.

Discussion

Although FRRf has previously been used for in situ estimation of GP, over a wide range of temporal and spatial scales,

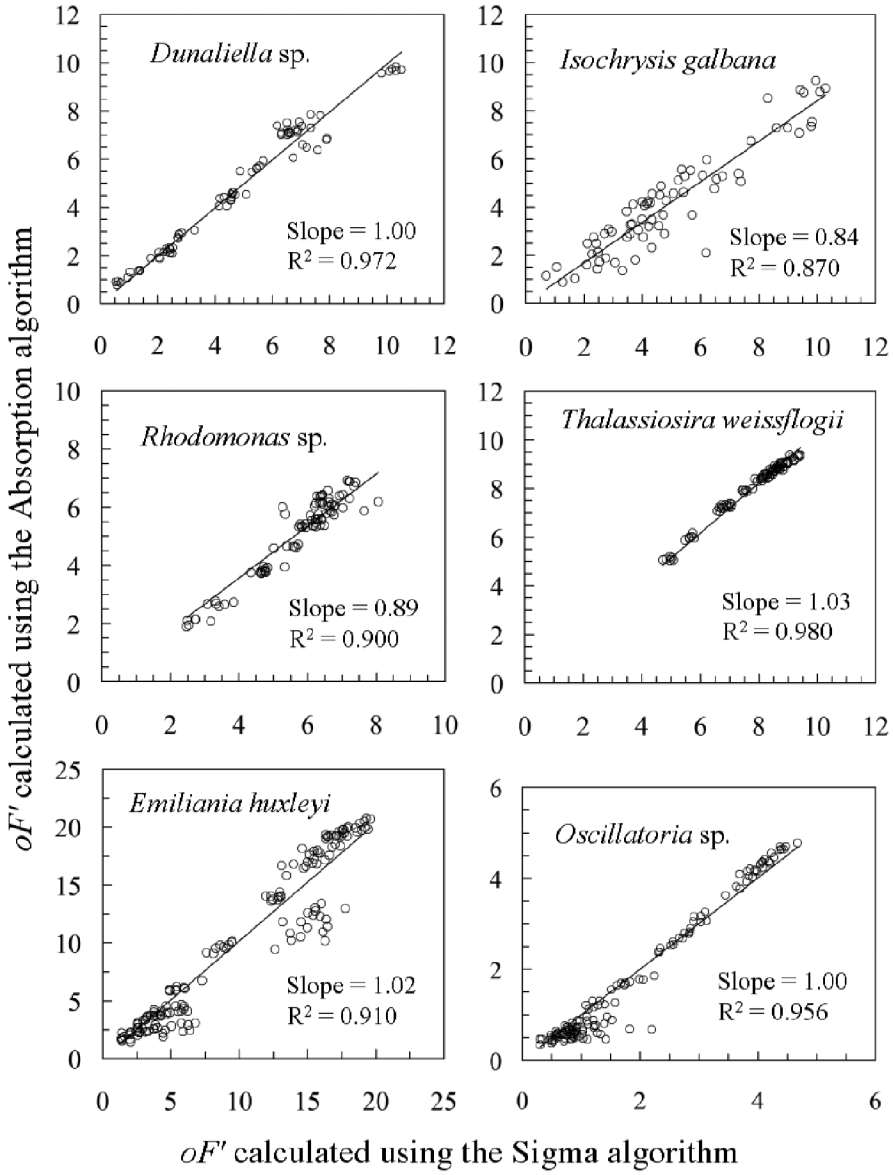

Fig. 5. Values of *oF'* calculated using the Sigma algorithm or Absorption algorithm. All measurements were made on cultures of the stated phytoplankton. In all cases, the regression lines were forced through the origin.

the requirement for an independent method to estimate [RCII] has greatly increased the time, effort, and cost of employing FRRf in this way (Moore et al. 2006; Suggett et al. 2006). This is particularly true when FRRf is used in situ, where variability through a profile or across a transect can greatly increase the number of [RCII] estimates required to generate reliable data.

As an alternative to using an independent method to estimate [RCII], we provide evidence of a strong correlation between [RCII] and F_o/σ_{PSII} (Figs. 3 and 4), which allows [RCII] to be estimated from dark FRRf measurements, alone. Although these data represent a limited number of phytoplankton species and environmental conditions, they provide significant evidence in favor of the underlying premise of this study: that k_p/k_f falls within a narrow range, for a wide range of phytoplankton groups, and potentially, under a wide range of environmental conditions.

Applying Eq. 10a to the calculation of [RCII] allows the sigma algorithm to be used to generate values for JV_{PSII}, without the requirement for an independent method to estimate [RCII]. Although this represents a significant advance, in terms of using FRRf to estimate GP and GPP, the absorption algorithm would seem to be a better choice. To summarize the advantages of the absorption algorithm:

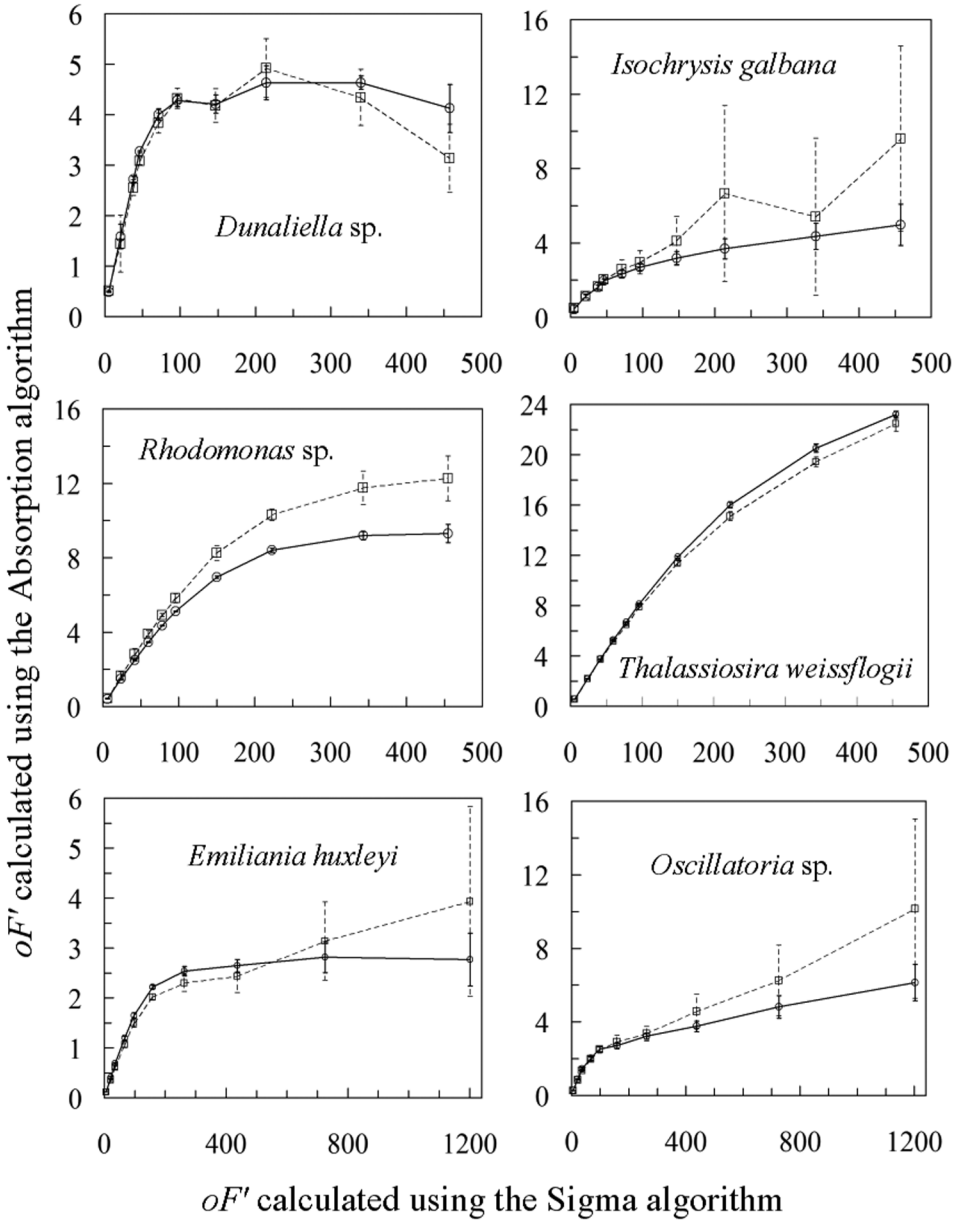

Fig. 6. Values of $oF' \cdot E$, calculated using the sigma algorithm (open squares, dashed lines) and absorption algorithm (open circles, solid lines) plotted against E. Shown are the mean values, plus 95% confidence intervals for $n = 6$.

There is no absolute requirement for an iterative fit to the kinetics of an ST acquisition

An iterative fit to a non-linear fluorescence transient is required when using the Sigma algorithm, to generate values for σ_{PSII} and σ_{PSII}'. In contrast, the Absorption algorithm requires only values of F_o, F_m, F' and F_m' (Eq. 13). In most situations, values for all four parameters are best derived using linear regression. In the case of F_o or F', regression through the first few points of an ST acquisition allows calculation of F_o or F' as the intercept (zeroth flashlet). In the case of F_m or F_m', regression through the last few points of an ST acquisition allows estimation of F_m or F_m' through extrapolation to the last flashlet. In situations where E_{LED} is well below the optimum value, estimation of F_m or F_m' as the asymptote of an iterative fit to an ST acquisition can be the best option. However, this only is true in extreme situations. For example, the data within Fig. 7 show only a minimal difference between the asymptote and regression values for F_m, even when E_{LED} is approximately 50% of the optimum value.

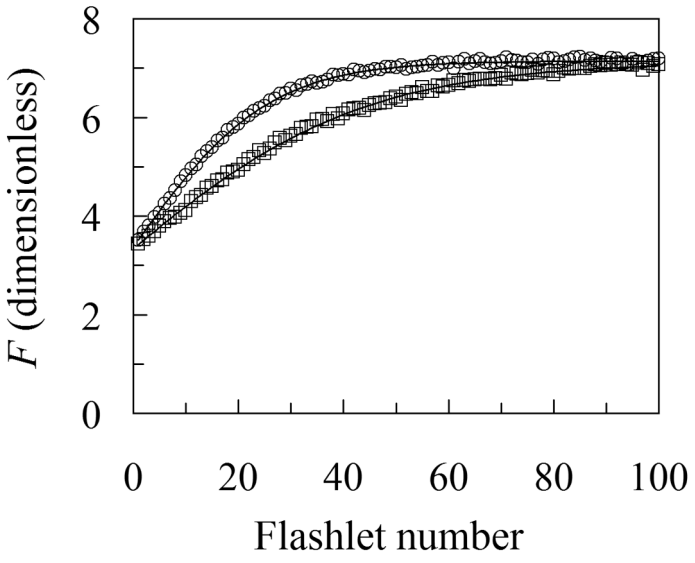

Fig. 7. ST acquisitions from a dark-adapted, optically thin static sample of *Chlorella* sp. Both acquisitions comprise 24 sequences, collected with 100 ms between adjacent sequences. One microsecond flashlets were delivered on a 2 µs pitch, giving a total time of 200 µs for each sequence. Each symbol represents an average from the 24 sequences. The solid lines are iterative fits through the entire ST curve (Kolber et al. 1998). The E_{LED} values were 0.63 x 10^{22} and 1.2 x 10^{22} photons m^{-2} s^{-1} (open squares and open circles, respectively). Asymptote and regression F_m values were 7.15 [7.04] and 7.17 [7.19] for the low and high E_{LED} values, respectively (regression values in brackets).

The algorithm is more consistent with assumptions concerning photosynthetic architecture

The sigma algorithm assumes uniform connectivity among RCIIs for calculation of both σ_{PSII}' and 1 – *C*, whereas calculation of 1 – *C* also requires that an assumption is made about the degree of connectivity (see Web Appendix A). Although connectivity-related errors are unlikely to be large (it would require an unusual combination of factors for the total error to exceed 15%), they are, in theory at least, completely negated by the absorption algorithm.

The measurement uncertainty is much lower

The most obvious benefit of not requiring σ_{PSII}' or 1 – *C* is the significantly increased precision of calculated parameter values at high *E*. For example, the values of $oF' \cdot E$ calculated using the sigma algorithm in Fig. 6 show much higher levels of uncertainty than the same values calculated, from the same data, using the absorption algorithm. This is very likely to result in more reliable values of JV_{PSII} at high *E* levels.

Applicability of the new approach

Although the absorption algorithm provides significant advantages over the Sigma algorithm, it does not resolve all of the issues associated with the FRRf method. Of particular note are the continued requirement for spectral correction of FRRf data (to account for differences in both the absorption characteristics of the phytoplankton and the spectral characteristics of available ambient light) and the need to assess the potential contribution of baseline fluorescence to the overall fluorescence signal. Whilst lack of spectral correction can result in very large errors, of 200% or more in some instances (Moore et al. 2006), they are consistent between the sigma and absorption algorithms, and are not discussed here. In contrast, the issue of baseline fluorescence is more complex.

We define baseline fluorescence as fluorescence emitted from sources other than functional RCIIs, which could include emission from any combination of the following: (1) LHIIs within the thylakoid membrane that are not connected to active RCIIs, (2) photosystem I (PSI), and (3) fluorescent dissolved organic matter within the sample volume.

Because, by definition, baseline fluorescence is nonvariable, it will contribute equally to the fluorescence signal at all points between F_o and F_m. In terms of the sigma algorithm (Eq. 2), baseline fluorescence has no impact on the value of $\sigma_{PSII}^{(\prime)}$ or the calculation of 1 – *C*, using qP, qL, or qJ, but would lead to a proportional overestimate of [RCII], if this value is calculated using Eq. 10a. For example, if baseline fluorescence added 10% to the fluorescence signal at F_o, this would result in a 10% overestimate of [RCII] and, by extrapolation, of JV_{PSII}. Given that a high proportion of baseline fluorescence is likely to originate from Chl *a* that is not functionally coupled to active RCIIs, it seems unlikely that direct measurement of Chl *a* concentration (the most commonly used alternative to Eq. 10a) would improve on this figure.

The absorption algorithm is also sensitive to baseline fluorescence. Within Eq. 13, baseline fluorescence would increase the value of $F_m \cdot F_o / (F_m - F_o)$ in proportion to the increase in F_o. Although the resulting overestimate of JV_{PSII} can be partly offset by a parallel decrease in the value of F_q'/F_m' (resulting from a higher value for k_d during the ambient light measurement), the latter is unlikely to be more than a few percent of the former, in most situations.

Differences in k_p/k_f between calibration and field samples could also introduce a proportional error to the value of JV_{PSII}. For example, a 50% suppression of k_p, between calibration and field sample, would result in a 100% overestimate of JV_{PSII}. As far as we are aware, there is no direct evidence for variability of this ratio within the published literature, and certainly the limited data presented within this study do not provide any such evidence. However, it has been suggested that low values of F_v/F_m observed under nutrient stress (particularly iron stress) could involve suppression of k_p (Vassiliev et al. 1995).

The suppression of F_v/F_m under nutrient stress can be very significant. For example, a number of studies in large, iron-limited ocean regions have indicated a doubling in the value of this parameter when iron was supplied; typically, from a value of around 0.3 to 0.6 (Behrenfeld et al. 1996; Boyd and Abraham 2001; Behrenfeld et al. 2004; Moore et al. 2007). From the discussion above, we can define three potential mechanisms that could result in suppression of F_v/F_m: baseline fluorescence, a decrease in k_p, and an increase in k_d. If the entire suppression of F_v/F_m is attributed to baseline fluores-

cence, this would require that approximately 70% of the fluorescence signal at F_o is baseline fluorescence, which would result in a 250% overestimate of JV_{PSII}, using Eq. 10a to calculate [RCII] within the sigma algorithm or using the absorption algorithm to calculate JV_{PSII} directly. If the entire suppression of F_v/F_m is attributed to a decrease in k_p the error would be an overestimate of approximately 400%. Conversely, if the entire suppression of F_v/F_m is attributed to a higher value for k_d in the dark-adapted state, the error would be zero. Clearly, there is a requirement for further study in this area, involving parallel application of FRRf and direct measurement of [RCII] and/or JV_{PSII}, to assess the validity of Eq. 10a and the absorption algorithm in such situations and, if required, to generate robust methods for correcting JV_{PSII} values.

It should be noted that, in the above example, the very large overestimate of JV_{PSII} resulting from a decrease in k_p is based on the definition of k_p as is the intrinsic rate constant for photochemistry within active RCIIs. Suppression of the average k_p among all RCII within the sample through RCII inactivation (such that k_p remains the same at some centers and is zero at others) would generate the smaller error associated with baseline fluorescence.

Overall, from the evidence presented within this article, we suggest that the following statements provide a reasonable summation of the new approach to the analysis of FRRf.

JV_{PSII} will be proportional to the fluorescence emitted by open RCII, providing the value of k_p/k_f remains close to the value within the calibration sample.

Suppression of F_v/F_m through an increase in k_d does not affect the calculation of JV_{PSII} using the absorption algorithm or of [RCII] using Eq. 10a.

The contribution of sources other than open RCIIs to F_o will result in an approximately proportional overestimate of JV_{PSII}.

Comments and recommendations

We started out with a very simple hypothesis; that under a given set of environmental conditions, k_p/k_f falls within a narrow range, for all groups of phytoplankton. Although the data presented here do not prove the universality of this assumption, there is overwhelming evidence within the literature to show that this basic premise holds true on a smaller scale (during a PE curve on a single sample, for example). In addition, the data from the BB and HP studies (Figs. 3 and 4) provide strong evidence that, even in a worst case scenario, only a small number of direct measurements of JV_{PSII} would be required to make use of this approach, on relatively large spatial and temporal scales.

Even if additional work shows that k_p/k_f varies significantly, the absorption algorithm would seem to provide a more practical method for assessing GP and GPP which, from the data presented within Fig. 6, would seem to extend the dynamic range of FRR, particularly within oligotrophic waters. However, the potential for overestimation of JV_{PSII} within nutrient stressed systems, due to baseline fluorescence and/or suppression of k_p, clearly needs to be assessed.

For the immediate future, the advent of the absorption method does not have any operational consequences for either laboratory-based or field-based studies, as both algorithms require FRRf data from measurements made under ambient light and dark-adapted conditions. Consequently, there seems no reason not to incorporate and compare data from both algorithms in any estimation of GP or GPP.

On a final note, it would seem worthwhile to work toward a situation where FRR fluorometers of a particular design (same spectral characteristics for the excitation LEDs and fluorescence detection system) are cross-calibrated to a set of universal standards (one or more species assayed using well-defined, independent methods for assessing [RCII] and/or JV_{PSII}). This would involve a series of detailed measurements being made on each fluorometer type, plus cross calibration among fluorometers of the same type through the K_N parameter.

References

Baker, N. R., and K. Oxborough. 2004. chlorophyll fluorescence as a probe of photosynthetic productivity, p. 65-82. *In* G. C. Papageorgiou and Govindjee [eds.], Chlorophyll *a* fluorescence: A signature of photosynthesis. Springer.

Begon, M., C. R. Townsend, and J. L. Harper. 2006. Ecology: From individuals to ecosystems, 4th ed. Blackwell.

Bender, M., and others. 1987. A comparison of four methods for determining plankton community production. Limnol. Oceanogr. 32:1085-1098 [doi:10.4319/lo.1987.32.5.1085].

Behrenfeld, M. J., A. J. Bale, Z. S. Kolber, J. Aiken, and P. G. Falkowski. 1996. Confirmation of iron limitation of phytoplankton photosynthesis in the equatorial Pacific Ocean. Nature 383:508-511 [doi:10.1038/383508a0].

———, O. Prasil, M. Babin, and F. Bruyant. 2004. In search of a physiological basis for covariations in light-limited and light saturated photosynthesis. J. Phycol. 40:4-25 [doi:10.1046/j.1529-8817.2004.03083.x].

———, K. Worthington, R. M. Sherrell, F. P. Chavez, P. Strutton, M. McPhaden, and D. M. Shea. 2006. Controls on tropical Pacific Ocean productivity revealed through nutrient stress diagnostics. Nature 442:1025-1028 [doi:10.1038/nature05083].

Boyd, P. W., and E. R. Abraham. 2001. Iron-mediated changes in phytoplankton photosynthetic competence during SOIREE. Deep-Sea Res. II 48:2529-2550.

Falkowski, P. G., and D. A. Kiefer. 1985. Chlorophyll *a* fluorescence in phytoplankton: Relationship to photosynthesis and biomass. J. Plankton Res. 7:715-731 [doi:10.1093/plankt/7.5.715].

———, D. Ziemann, Z. Kolber, and P. K. Bienfang. 1991. Role of eddy pumping in enhancing primary production in the ocean. Nature 352:55-58 [doi:10.1038/352055a0].

Fogg, G. E., and O. Calvario-Martinez. 1989. Effects of bottle size in determinations of primary productivity by phytoplankton. Hydrobiologia 173:89-94 [doi:10.1007/BF00015518].

Geider, R. J., and H. L. Macintyre. 2002. Physiology and biochemistry of photosynthesis and algal carbon acquisition. *In* P. J. le B. Williams, D. N. Thomas, and C. S. Reynolds [eds.], Phytoplankton productivity. Blackwell Science, London. [doi:10.1002/9780470995204.ch3].

Genty, B., J.-M. Briantais, and N. R. Baker. 1989. The relationship between the quantum yield of photosynthetic electron transport and quenching of chlorophyll fluorescence. Biochim. Biophys. Acta 990:87-92 [doi:10.1016/S0304-4165(89)80016-9].

Halsey, K. H., A. J. Milligan, and M. J. Behrenfeld. 2010. Physiological optimization underlies growth rate-independent chlorophyll-specific gross and net primary production. Photosynth. Res. 103:125-137 [doi:10.1007/s11120-009-9526-z].

Havaux, M., R. J. Strasser, and H. Greppin. 1991. Effect of incident light intensity on the yield of steady state chlorophyll fluorescence in intact leaves. Environ. Exp. Bot. 31:23-32 [doi:10.1016/0098-8472(91)90004-8].

Joliot, A., and P. Joliot. 1964. Etude cinétique de la reaction photochimique libérant l'oxygèn au cours de la photosynthèse. C.R. Acad. Sci. (Paris) 143:4622-4625.

Kolber, Z. S., and P. G. Falkowski. 1993. Use of active fluorescence to estimate phytoplankton photosynthesis in situ. Limnol. Oceanogr. 38:1646-1665 [doi:10.4319/lo.1993.38.8.1646].

———, O. Prásîl, and P. G. Falkowski. 1998. Measurements of variable chlorophyll fluorescence using fast-repetition rate techniques: defining methodology and experimental protocols. Biochim. Biophys. Acta 1367:88-106 [doi:10.1016/S0005-2728(98)00135-2].

Krause, G. H., and P. Jahns. 2004. Non-photochemical energy dissipation determined by chlorophyll fluorescence quenching: characterization and function, p. 463-495. *In* G. C. Papageorgiou and Govindjee [eds.], Chlorophyll *a* fluorescence: A signature of photosynthesis. Springer.

Kramer, D. M., G. Johnson, O. Kiirats, and G. E. Edwards. 2004. New fluorescence parameters for the determination of QA redox state and excitation energy fluxes. Photosynth. Res. 27:41-55.

Lavergne, J., and H. W. Trissl. 1995. Theory of fluorescence induction in photosystem. II. Derivation of analytical expressions in a model including exciton-radical-pair equilibrium and restricted energy-transfer between photosynthetic Units. Biophys. J. 68:2474-2492 [doi:10.1016/S0006-3495(95)80429-7].

Lazár, D. 1999. Chlorophyll *a* fluorescence induction. Biochim. Biophys. Acta 1412:1-28 [doi:10.1016/S0005-2728(99)00047-X].

Moore, C. M., and others. 2003. Physical controls on phytoplankton physiology and production at a shelf sea front: a fast repetition-rate fluorometer based field study. Mar. Ecol. Progr. Ser. 259:29-45.

———, D. J. Suggett, A. E. Hickman, Y.-N. Kim, J. Sharples, R. J. Geider, and P. M. Holligan. 2006. Phytoplankton photoacclimation and photo-adaptation in response to environmental gradients in a shelf sea. Limnol. Oceanogr. 51:936-949 [doi:10.4319/lo.2006.51.2.0936].

———, and others. 2007. Iron-light interactions during the CROZet natural iron bloom and EXport experiment (CROZEX) I: Phytoplankton growth and photophysiology. Deep-Sea Res. II 54:2045-2065 [doi:10.1016/j.dsr2.2007.06.011].

Oxborough, K., and N. R. Baker. 1997. Resolving Chlorophyll *a* fluorescence images of photosynthetic efficiency into photochemical and non-photochemical components—calculation of qP and Fv′/Fm′ without measuring Fo′. Photosynth. Res. 54:135-142 [doi:10.1023/A:1005936823310].

Raven, J. A. 2009. Functional evolution of photochemical energy transformations in oxygen-producing organisms. Funct. Plant Biol. 36:505-515 [doi:10.1071/FP09087].

Shoaf, W. T., and B. W. Lium. 1976. Improved extraction of Chlorophyll *a* and *b* from algae using dimethyl sulfoxide. Limnol. Oceanogr. 21:926-928 [doi:10.4319/lo.1976.21.6.0926].

Suggett, D. J., G. Kraay, P. Holligan, M. Davey, J. Aiken, and R. J. Geider. 2001. Assessment of photosynthesis in a spring cyanobacterial bloom by use of an FRR fluorometer. Limnol. Oceanogr. 46:802-810 [doi:10.4319/lo.2001.46.4.0802].

———, K. Oxborough, N. R. Baker, H. L. MacIntyre, T. M. Kana, and R. J. Geider. 2003. Fast Repetition Rate and Pulse Amplitude Modulation Chlorophyll *a* fluorescence measurements for assessment of photosynthetic electron transport in marine phytoplankton. Eur. J. Phycol. 38:371-384 [doi:10.1080/09670260310001612655].

———, H. L. MacIntyre, and R. J. Geider. 2004. Evaluation of biophysical and optical determinations of light absorption by photosystem II in phytoplankton. Limnol. Oceanogr. Methods 2:316-332 [doi:10.4319/lom.2004.2.316].

———, S. H. Maberly, and R. J. Geider. 2006. Gross photosynthesis and lake community metabolism during the spring phytoplankton bloom. Limnol. Oceanogr. 51:2064-2076 [doi:10.4319/lo.2006.51.5.2064].

———, H. L. MacIntyre, T. M. Kana, and R. J. Geider. 2009a. Comparing electron transport with gas exchange: parameterising exchange rates between alternative photosynthetic currencies for eukaryotic phytoplankton. Aquatic Microb. Ecol. 56:147-162 [doi:10.3354/ame01303].

———, C. M. Moore, A. E. Hickman, and R. J. Geider. 2009b. Interpretation of Fast Repetition Rate (FRR) fluorescence: signatures of community structure v physiological state. Mar Ecol. Prog. Ser. 376:1-19 [doi:10.3354/meps07830].

———, C. M. Moore, and R. J. Geider. 2010a. Estimating aquatic primary productivity using active fluorescence, p. 103-128. *In* D. J. Suggett, O. Prasil, and M. A. Borowitzka [eds.], Chlorophyll *a* fluorescence in aquatic sciences: methods and applications. Springer.

———, O. Prá_il, and M. A. Borowitzka. 2010b. Chlorophyll *a*

fluorescence in aquatic sciences: methods and applications. Springer [doi:10.1007/978-90-481-9268-7].

Vassiliev, I. R., Z. Kolber, K. D. Wyman, D. Mauzerall, V. K. Shukla, and P. G. Falkowski. 1995. Effects of iron limitation on photosystem. II. Composition and light utilization in *Dunaliella-tertiolecta*. Plant Physiol. 109:963-972.

Venrick, E. L., J. R. Beers, and J. F. Heinbokel. 1977. Possible consequences of containing microplankton for physiological rate measurements. J. Exp. Mar. Biol. Ecol. 26:55-76 [doi:10.1016/0022-0981(77)90080-6].

Welschmeyer, N. A. 1994. Fluorometric analysis of chlorophyll *a* in the presence of chlorophyll band pheopigments. Limnol. Oceanogr. 39:1985-1992 [doi:10.4319/lo.1994.39.8.1985].

Submitted12 January 2012
Revised 6 February 2012
Accepted 13 February 2012